



Investigating the Antifungal Activity of *Embelia ribes* extracts Against *Candida albicans*: A Computational Approach

Asweshvaran R¹, Rakesh Kumar Yadav¹, Satheesh Kumar S¹, Harathi C¹, Malaiyarasa Pandian², Yuvaraj Ponnusamy¹, KN Chandrashekara¹, and Guru Prasad V¹

¹ Shriram Research Institute, Bengaluru, Karnataka, India 560048

² Department of life Sciences-Microbiology, Indian Academy Degree College- Autonomous, Bengaluru, Karnataka, India

Asweshvaran R, Rakesh Kumar Yadav, Satheesh Kumar S, Harathi C, Malaiyarasa Pandian, Yuvaraj Ponnusamy, KN Chandrashekara, Guru Prasad V 2026 – Investigating the Antifungal Activity of *Embelia ribes* extracts Against *Candida albicans*: A Computational Approach. Current Research in Environmental & Applied Mycology (Journal of Fungal Biology) 16(1), 32–45, Doi 10.5943/cream/16/1/3

Abstract

The emergence of antifungal resistance in *Candida albicans* necessitates the development of alternative therapeutic agents. This study evaluated the antifungal properties of *Embelia ribes* extracts using both *in silico* and *in vitro* approaches. Fresh and dry seeds were extracted using solvents of varying polarity and analyzed via GC-MS/MS. Results indicated that the fresh methanolic extract (FERM) exhibited superior antifungal activity with a zone of inhibition of 21.6 ± 0.5 mm, which was statistically equivalent to the positive control (Clotrimazole, 22.0 ± 1.0 mm). Bioactive profiling identified Piperine (24.07%) as the primary constituent in the most active extract. Molecular docking revealed that Piperine and Dipiperonylamine possess strong binding affinities for Cyclooxygenase-2 and Kappa-opioid receptors, suggesting a dual antifungal and anti-inflammatory mechanism. Pharmacokinetic profiling (ADME/T) confirmed favourable drug-like properties, however, low CNS permeability limits their utility to the treatment of peripheral infections. These findings position *E. ribes* as a promising source for the development of novel antifungal drugs.

Keywords – ADMET – Antifungal – COX 2 – Dipiperonylamine – Piperine

Introduction

Candida species (Kingdom: Fungi; Phylum: Ascomycota; Class: Saccharomycetes; Order: Saccharomycetales; Family: Debaryomycetaceae) are commensal fungi present in approximately 40–60% of the general population, colonizing the gastrointestinal tract, oral cavity, and other mucosal surfaces (Jeziorek et al. 2019). Under favorable conditions, these fungi can transition into opportunistic pathogens, leading to infections influenced by risk factors such as prolonged antibiotic use, chronic alcohol consumption, immunosuppressive therapy, and high-carbohydrate diets (Ghany et al. 2024). *Candida* infections range from superficial mucosal involvement to deep-seated systemic diseases, with resistance to antifungal agents emerging as a major clinical concern (Wang et al. 2024). This resistance arises through genetic mutations and adaptive mechanisms induced by prolonged antifungal exposure, complicating treatment strategies (Ghany et al. 2024).

The increasing prevalence of azole-resistant *Candida* strains underscores the urgent need for novel antifungal therapies. (Ghany et al. 2024, Wang et al. 2024).

Triosephosphate isomerase (TPI), traditionally recognized as a glycolytic enzyme, has recently been identified as a structural component of the *Candida* yeast cell wall, where it plays a crucial role in fungal adhesion, facilitating colonization and infection (Satala et al. 2021). Dihydrofolate reductase (DHFR), an enzyme essential for nucleotide synthesis and cellular survival, remains a key therapeutic target for antimicrobial agents. However, the emergence of drug-resistant microorganisms underscores the need for novel DHFR inhibitors to enhance treatment efficacy (Ghany et al. 2024, Sehrawat et al. 2024).

Beyond microbial targets, host receptors such as kappa-opioid receptors (KOR) play a significant role in regulating physiological processes, including pain modulation and stress response. Despite their therapeutic potential, adverse effects have limited their clinical application. Cyclooxygenase (COX) enzymes, specifically COX-1 and COX-2, are critical mediators of inflammatory responses and are the primary targets of nonsteroidal anti-inflammatory drugs (NSAIDs). While COX-1 is constitutively expressed, COX-2 is rapidly upregulated during inflammation, making it a more relevant marker for inflammatory changes and a preferred target for selective anti-inflammatory interventions (Shrestha et al. 2020).

Embelia ribes, a woody climbing plant belonging to the family Primulaceae, is commonly referred to as false black pepper or Vaividang. The plant is rich in bioactive compounds, with embelin being its primary constituent, recognized for its broad-spectrum medicinal properties. Notably, *E. ribes* has demonstrated antifungal activity against *Candida albicans*, making it a promising natural agent for managing infections such as oral thrush, fungal dermatitis, and gastrointestinal candidiasis. Beyond its antifungal potential, *E. ribes* exhibits antibacterial, antioxidant, anti-inflammatory, and wound-healing properties, further supporting its therapeutic applications in infectious and inflammatory conditions (Leema Joseph et al. 2024, Patel et al. 2024, Prakash et al. 2024).

Despite the known medicinal properties of *E. ribes*, the comparative influence of seed condition (fresh versus dry) and solvent polarity on the extraction of bioactive antifungal metabolites remains underexplored. Therefore, the objectives of this study are to: (1) optimize the extraction of bioactive constituents from fresh and dry *E. ribes* seeds using solvents of varying polarity; (2) validate their antifungal efficacy against *C. albicans in vitro*; and (3) utilize GC-MS/MS profiling coupled with molecular docking and ADME/T analysis to identify lead compounds and elucidate their potential mechanisms of action against key fungal and inflammatory targets.

Materials & Methods

Collection of samples and Extraction Methods

Dried *E. ribes* seed powder was procured from SPS Marketing, Coimbatore, while fresh seeds were collected from Neerveli, Kannur, Kerala, India. For extraction, 25 g of dried (D) and fresh (F) *E. ribes* seed powder was separately immersed in 125 mL of ethyl acetate (EREA) and methanol (ERM) to isolate both semi-polar and polar bioactive constituents, sealed, and stored at 4°C for 10 days. Additionally, 25 g of fresh *E. ribes* seeds were coarsely powdered and extracted using 125 mL of chloroform (ERC) under reflux at 70°C for one hour to isolate non-polar lipophilic compounds. The extracts were centrifuged at 4000 rpm for 10 minutes to separate the plant material, and the supernatant was collected. Solvent evaporation yielded the concentrated extract, which was subsequently dissolved in 2 mL of the respective solvent. The chloroform extract was reconstituted in ethyl acetate (ERCE) with 2 mL of purifier (Bondesil-PSA, Agilent Technologies, USA) to eliminate matrix interferences such as fatty acids (Khetagoudar et al. 2022, Dela Peña et al. 2025). The prepared extracts were subjected to GC-MS/MS analysis and evaluated for their anticandidal activity.

GC-MS/MS Analysis

Gas chromatography-mass spectrometry (GC-MS/MS) was utilized to characterize the bioactive constituents of *E. ribes* in both dry and fresh extracts. The analysis was conducted using a Shimadzu GC-MS/MS TQ 8030 system, employing electron impact ionization (EI) for compound detection. A HP 5 MS capillary column (30 m × 0.25 mm × 0.25 μm) was used, with an optimized oven temperature program: an initial hold at 120°C for 2 minutes, followed by a temperature ramp of 15°C/min to 180°C (held for 1 minute), a subsequent increase of 5°C/min to 200°C (held for 1 minute), and a final ramp of 6°C/min to 290°C (held for 7 minutes), resulting in a total run time of 34 minutes. The injector temperature was programmed to increase at a rate of 80°C/min up to 290°C. Identification of bioactive compounds was achieved by comparing the obtained mass spectra with reference data from the National Institute of Standards and Technology (NIST) library. To ensure accuracy, compound identification was restricted to those exhibiting a spectral similarity index (SI) of ≥ 90% (Match Quality). Additionally, the experimental retention times (RT) were cross-referenced with literature values to validate the elution order of the identified constituents.

Table 1 GC-MS-MS Analysis conditions

Parameter	Details
Instrument Used	Shimadzu GC-MS/MS TQ 8030
Ionization Method	Electron Impact Ionization (EI)
Sample Type	Dry and fresh extracts of <i>Embelia ribes</i>
Capillary Column	HP 5 MS (30 m × 0.25 mm × 0.25 μm)
Oven Temperature Program	120°C for 2 min, 15°C/min to 180°C (held 1 min), 5°C/min to 200°C (held 1 min), 6°C/min to 290°C (held 7 min)
Total Run Time	34 minutes
Injector Temperature Program	80°C/min up to 290°C
Compound Identification	Comparison with NIST database spectra

Anticandidal Effect

Multiple colonies from the sub-cultured organism were transferred into 5 mL of sterile distilled water, followed by agitation for 15 seconds to ensure homogeneity. The suspensions were then adjusted to match the turbidity of a 0.5 McFarland standard and further diluted with sterile distilled water to obtain working suspensions of *Candida albicans* (MTCC 227), ranging from 1–5 × 10⁵ CFU/mL and 1–5 × 10³ CFU/mL for antifungal susceptibility testing. The antifungal activity of *E. ribes* (False black pepper) extracts was evaluated using the well diffusion method, with Clotrimazole (30 μg/well) serving as a positive control. The assay was performed in duplicate by introducing 100 μL of *E. ribes* extract (10 mg/well) into wells on Yeast Extract–Peptone–Glycerol Agar (YPGA) medium, followed by incubation to assess antifungal efficacy.

Ligands and macromolecule

Chemical data obtained from GC-MS/MS analysis were systematically integrated into the PubChem database using Python-based workflows, leveraging the PubChemPy and RDKit libraries (Tahlil et al. 2023). This process involved uploading experimental data to PubChem, retrieving corresponding Compound IDs (CIDs) and SMILES notations, and subsequently downloading 3D structure files in .sdf format. The integration of these chemical profiles into a widely accessible database facilitates further computational analysis, enabling broader applications in cheminformatics, drug discovery, and molecular docking studies (mcs07 2016).

ADME/T Properties

The ADME properties of compounds derived from *E. ribes* were evaluated using Swiss ADME and pkCSM, two *in silico* tools for predicting pharmacokinetic and physicochemical

characteristics. Swiss ADME, developed by the Swiss Institute of Bioinformatics (<http://www.swissadme.ch/>), utilizes SMILES notation to estimate key aspects of absorption, distribution, metabolism, excretion, and toxicity (ADME/T). Complementarily, pkCSM, a platform from the University of Queensland (<https://biosig.lab.uq.edu.au/pkcsm/prediction>), provides predictions on pharmacokinetics and pharmacodynamics. The integration of these computational approaches facilitates a comprehensive assessment of drug-like properties, supporting early-stage drug development and candidate optimization (Mazri et al. 2024, Sarwar et al. 2024).

Molecular docking study

Computational approaches were employed to evaluate the binding affinities of bioactive compounds identified in *E. ribes* seed extract against selected protein targets. Molecular docking studies were conducted using DockThor Version 2.0 (<https://dockthor.lncc.br/v2/>), along with structural visualization and refinement tools such as PyMOL (with drawgridbox.py), Discovery Studio, and Swiss PDB Viewer. The binding sites of each target protein were defined based on their reported active residues. For instance, triosephosphate isomerase (Tpi1) (UniProt ID: Q9P940) contained active regions spanning residues 4–17 (“QFFVGGNFKANGTK”) and 224–247 (“KANVDGFLVGGASLKPEFVDIIKSR”), with grid parameters set at center coordinates ($x = 3.4189\text{\AA}$, $y = -3.4305\text{\AA}$, $z = -18.585\text{\AA}$) and dimensions ($x = 20.918\text{\AA}$, $y = 27.917\text{\AA}$, $z = 26.954\text{\AA}$) at a discretization of 0.26 (Satala et al. 2021). Grid settings for additional protein targets, including glucose transporter 3 (GLUT3) (PDB ID: 4ZWB), dihydrofolate reductase (DHFR) (PDB ID: 4M6J), kappa opioid receptor (KOR) (PDB ID: 6VI4), and cyclooxygenase-2 (COX-2) (PDB ID: 1CX2), were adapted following the protocol by Taher et al. (2024). Docking simulations utilized a genetic algorithm with the following parameters: one million evaluations, a population size of 750, 24 independent runs, and an initial seed value of -1985. Before docking, native ligands were removed, and 24 binding modes were assessed for each compound. The selection of the most favorable ligand conformation was based on the lowest energy-minimized pose, with structural comparisons performed using root mean square deviation (RMSD) values. Interaction analysis of docking results was carried out using Discovery Studio 2016 Taher et al. (2024).

Data Analysis and Visualization

Experimental data were expressed as mean \pm SD ($n=3$). Statistical differences were evaluated using One-Way ANOVA followed by Dunnett’s t-test in IBM SPSS (v27.0) (Arafat et al. 2025). To elucidate metabolic distinctions, Principal Component Analysis (PCA) and Hierarchical Cluster Analysis (HCA) were performed in R using the factoextra and ggplot2 packages. GC-MS data matrices were log-transformed for normalization, with principal components selected via the Kaiser criterion (Eigenvalues > 1) to delineate significant chemometric variance and clustering patterns.

Results

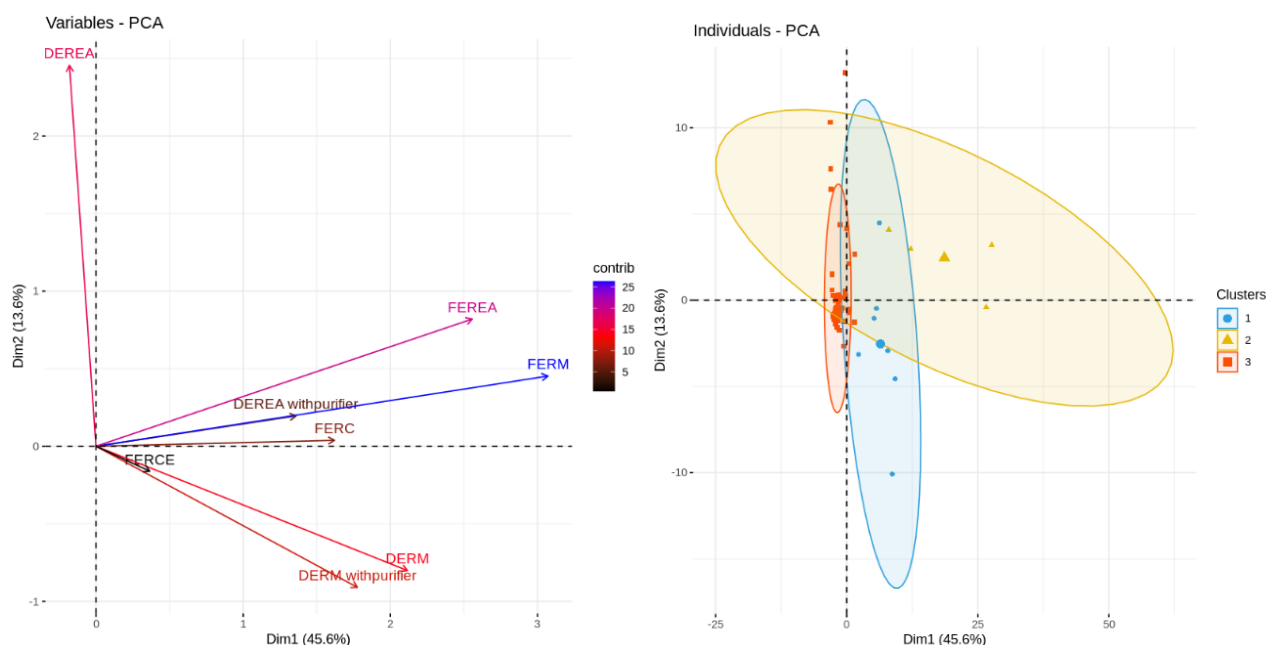
Chemical Composition

The GC-MS analysis of various extracts, namely DERE (Dry *E. ribes* ethyl acetate), DERM (Dry *E. ribes* methanol), FERM (Fresh *E. ribes* methanol), FER (Fresh *E. ribes* chloroform), FER (Fresh *E. ribes* ethyl acetate), and FERCE (Fresh *E. ribes* chloroform-ethyl acetate), reveals a plethora of chemical compounds present in each extract. These compounds encompass a wide range of chemical classes, including terpenoids, alkanes, acids, amides, and esters, among others. The DERE extract exhibited a significant presence of fatty acids, terpenes, and amides, indicating potential nutritional and bioactive properties. Notably, compounds like cis-10-Heptadecenoic acid and N-Isobutyl-11-(3,4-methylenedioxyphenyl)-2E,4E,10E-undecatrienoic amide showed high percentages, suggesting their potential therapeutic relevance. In contrast, the DERM extract with purifier displayed a different chemical profile, with notable compounds such as Piperine and Bicyclo[5.2.0] nonane derivatives, indicating potential bioactivity and flavoring properties. Similarly, the DERM extract exhibited a diverse chemical composition, with

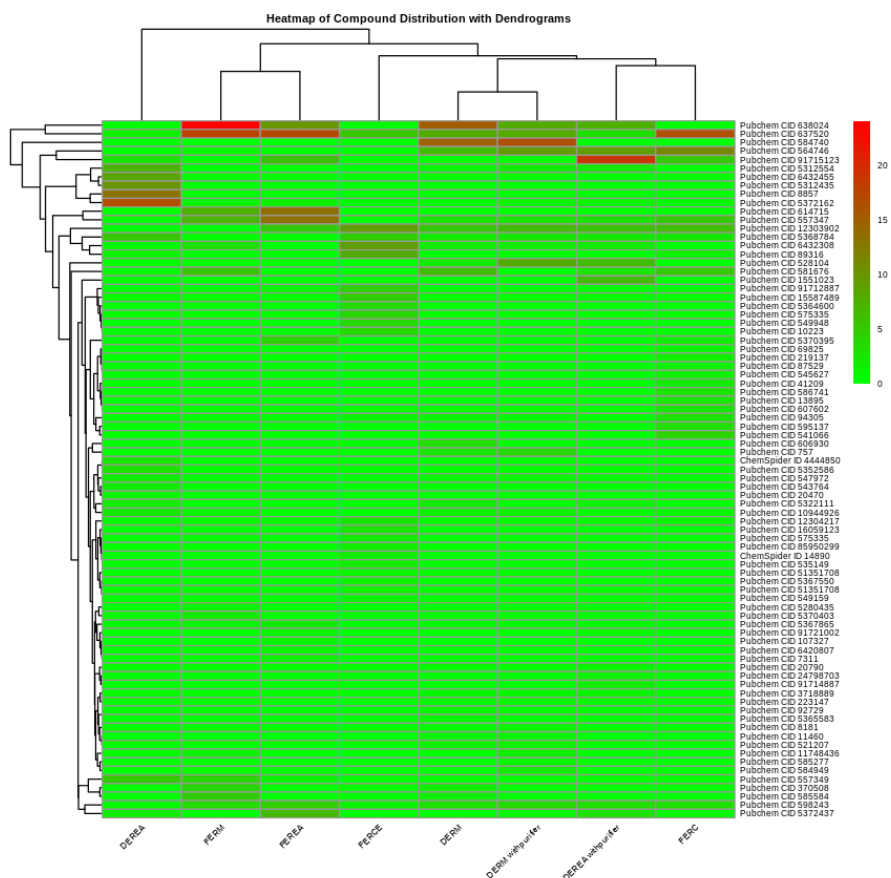
compounds such as Furazan-3-amine and Piperine present at high percentages, suggesting their potential pharmacological significance. The extracts with purifiers, including FERM, FERC, FEREA, and FERCE, displayed unique chemical profiles characterized by a variety of compounds with potential medicinal applications. Piperine and 2-Propenoic acid were prominent in these extracts, indicating their potential pharmacological activities. Molecule 23, identified as Piperine, exhibited the highest percentage area in the FERM extract (24.07%), followed by the DERM extract (15.17%). Molecule 114, identified as Di(3,4-methylenedioxybenzyl) amine or Dipiperonylamine, showed a percentage area in the DERM with purifier of 0.87%. Molecule 227, identified as Metathebainon or Dibenz[d,f]indol-2(5H)-one, 3,4,6,7,7a,8-hexahydro-12-hydroxy-11-methoxy-7-methyl-, [4aS-(4aR*,7aS*)]-, demonstrated a percentage area in the FERCE with purifier of 0.001%. The chemical analysis shown in Figure 1 of these extracts highlights their diverse composition.

A notable cluster of compounds exhibits higher activity levels (red) under the conditions labeled FERM and FEREA (Figs 1 B). These conditions appear to induce a distinct compound profile compared with other conditions. Most compounds exhibit low activity (green) across the majority of conditions, with a few exceptions showing moderate levels (brown/yellow). The conditions labeled DERM, FERCE, and DERM with purifier display relatively uniform compound distributions with minimal variability, as indicated by the consistent green color. In contrast, conditions FERM and FEREA show more significant variability, suggesting these conditions might be influencing the metabolic or chemical pathways leading to the production or activation of specific compounds.

The first two principal components (Dim1 and Dim2) were selected using the Kaiser criterion (Eigenvalues > 1), as they accounted for the most variance in the dataset. Together, Dim1 (45.6%) and Dim2 (13.6%) explained 59.2% of the total cumulative variance. The variables plot (Figs 1 A) indicates that FERM and FEREA contributed most strongly to the variation in Dim1 and Dim2. In the individuals plot, the samples formed distinct groups: Cluster 2 (Yellow) contained the fresh extracts, while Clusters 1 and 3 comprised the dry extracts (DERM, DERE), showing a clear visual separation between fresh and dry samples (Figs 1 A).



Figs 1 – A Dry and Fresh *E. ribes* seeds show the principal components analysis (PCA) plot of Dim1 vs Dim2. Colors and symbols represent different Extract and chemical respectively.



Figs 1 – B Percentage of chemicals in *E. ribes* extracts, those chemical labels are PubChem CID and Chemspider ID numbers. Values are the logarithmic transformed fold change (32 to 0). Different colors represent the increase or decrease in percentage of chemicals in extract logarithmic fold change as indicated in the color index.

In Silico

ADMET

A total of 240 chemical compounds were analyzed. Molecule 23, Molecule 114, and Molecule 227 all successfully passed the Lipinski rule without any violations as shown in Table 2. This determination was made based on various parameters, including molecular weight below 500, LogP, hydrogen bond donors, rotatable bonds, and hydrogen bond acceptors, all of which contribute to assessing drug permeability and efficacy. Notably, Molecule 23 exhibited violations under the Brenk criteria, specifically regarding Michael acceptor 1 and polyene. Therefore, 120 molecules were clear without violation, but have violation of other criteria of Ghose, Veber, Egan, Muegge, PAINS, Brenk, and Leadlikeness.

Table 2 Molecule 23, 114, 227 shows the complies with the Lipinski rule

Molecule no.	Molecule 23	Molecule 114	Molecule 227	Lipinski rules
Molecular Weight	285.343	285.299	299.37	≤ 500 Da
Log P	2.9972	2.4338	2.3937	≤ 5
Rotatable Bonds	3	4	1	Not define
Acceptors	3	5	4	≤ 10
Donors	0	1	1	≤ 5
Surface Area (Å ²)	124.203	121.941	129.933	Not define

All three molecules demonstrated excellent intestinal uptake, with Caco-2 permeability coefficients exceeding 0.9 and predicted human intestinal absorption above 90%, yet all three showed low skin permeability ($\log K_p < -2.5$). In their metabolic profiles, Molecule 227 was identified as a CYP2D6 inhibitor and a substrate of CYP3A4, Molecule 23 as a CYP2C19 inhibitor and CYP3A4 substrate, and Molecule 114 as a CYP1A2 inhibitor. Distribution metrics revealed that Molecule 227 has a high steady-state volume of distribution ($VD_{ss} = 1.27 \log L/kg$) and moderate blood–brain barrier penetration, whereas Molecules 23 and 114 exhibited medium VD_{ss} and were capable of crossing into the central nervous system, albeit with low CNS permeability. Clearance rates varied from 0.24 $\log mL/min/kg$ for Molecule 23 to 0.908 $\log mL/min/kg$ for Molecule 227 and 1.207 $\log mL/min/kg$ for Molecule 114. Finally, none of the compounds showed skin sensitization potential, and all returned negative results in the Ames test, indicating a low likelihood of genotoxicity.

Table 3 Absorption, Distribution, Metabolism, Excretion, and Toxicity of molecules

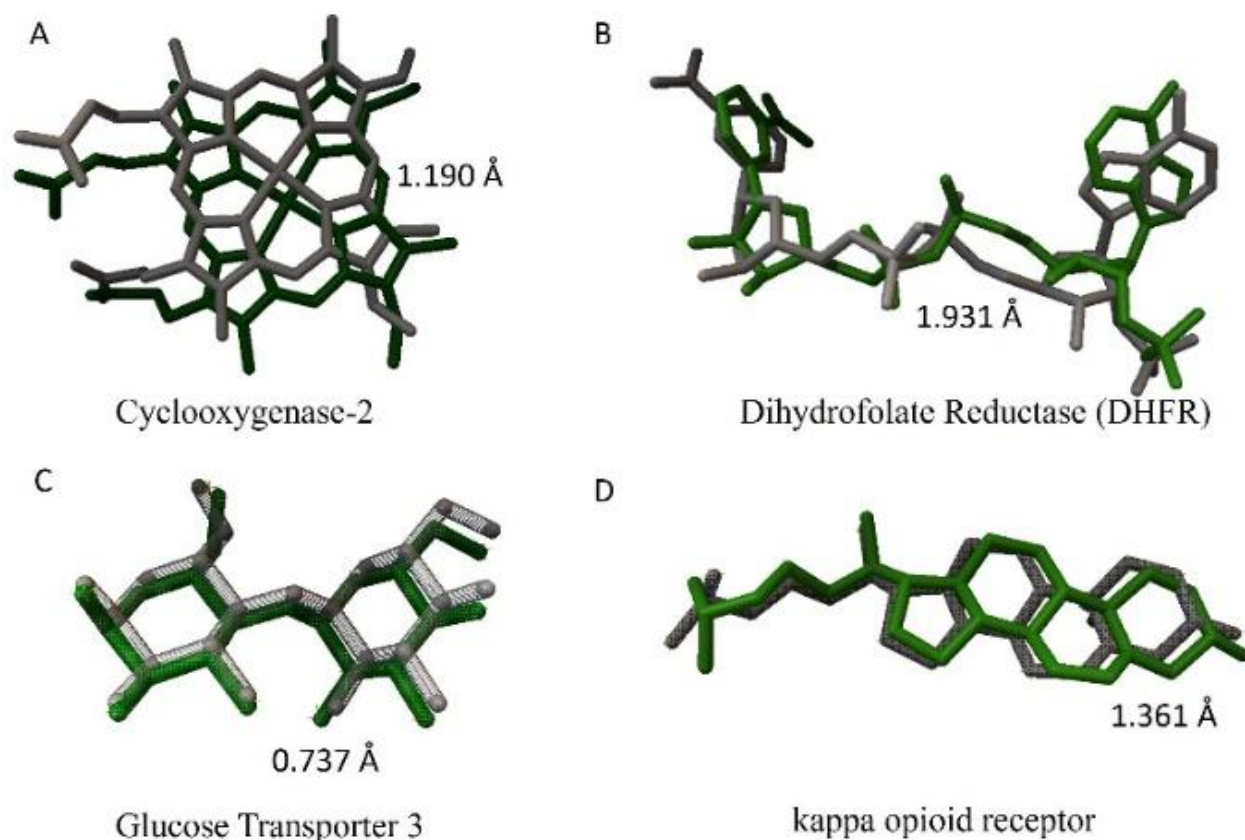
Parameter/Molecules No.	23	114	227
CaCo2 permeability	1.893	1.297	1.253
Intestinal absorption (human)	94.355	94.083	91.74
Skin Permeability	-2.819	-2.624	-2.828
VD_{ss} (human)	0.268	0.694	1.27
BBB permeability	0.274	0.272	0.133
CNS permeability	-1.625	-1.926	-2.114
CYP2D6 substrate	No	No	No
CYP3A4 substrate	Yes	Yes	No
CYP1A2 inhibitor	No	Yes	No
CYP2C19 inhibitor	Yes	No	No
CYP2C9 inhibitor	No	No	No
CYP2D6 inhibitor	No	No	Yes
CYP3A4 inhibitor	No	No	No
Total Clearance	0.24	1.207	0.908
Skin Sensitisation	No	No	No

Autodocking

All docked complexes exhibited RMSD values below 2 Å, confirming the reproducibility and reliability of binding poses. The binding energies and molecular interactions observed across all targets further validate the docking protocol and suggest stable, biologically relevant ligand–target complexes (Figs 2 A-D).

The interaction analysis of selected protein–ligand complexes revealed significant non-covalent interactions contributing to complex stability and affinity scores are shown on Table 4. The DHFR–Metathebainon complex (Figs 3 A) exhibited stability primarily through a conventional hydrogen bond with SER A:116, along with alkyl and π -alkyl interactions involving LYS A:53, TYR A:119, and ILE A:14. Although an unfavorable acceptor–acceptor interaction was noted with ILE A:14, the overall interaction network was sufficient to maintain complex integrity. The COX-2–Dipiperonylamine complex (Figs 3 B) displayed stability due to conventional hydrogen bonds with ARG A:481 and HIS A:58, as well as extensive non-covalent interactions. This included van der Waals forces, carbon–hydrogen bonds, and π -alkyl interactions with LEU A:320 and ALA A:495. Additional alkyl bonds with TYR A:353, TRP A:355, and ALA A:484 enhanced ligand stabilization within the active site. The GLUT3–Metathebainon complex (Figs 3 C) was stabilized through a conventional hydrogen bond with VAL A:65, a π -donor hydrogen bond with ALA A:66, and a carbon–hydrogen bond with ASN A:284. Further support was provided by alkyl and π -alkyl

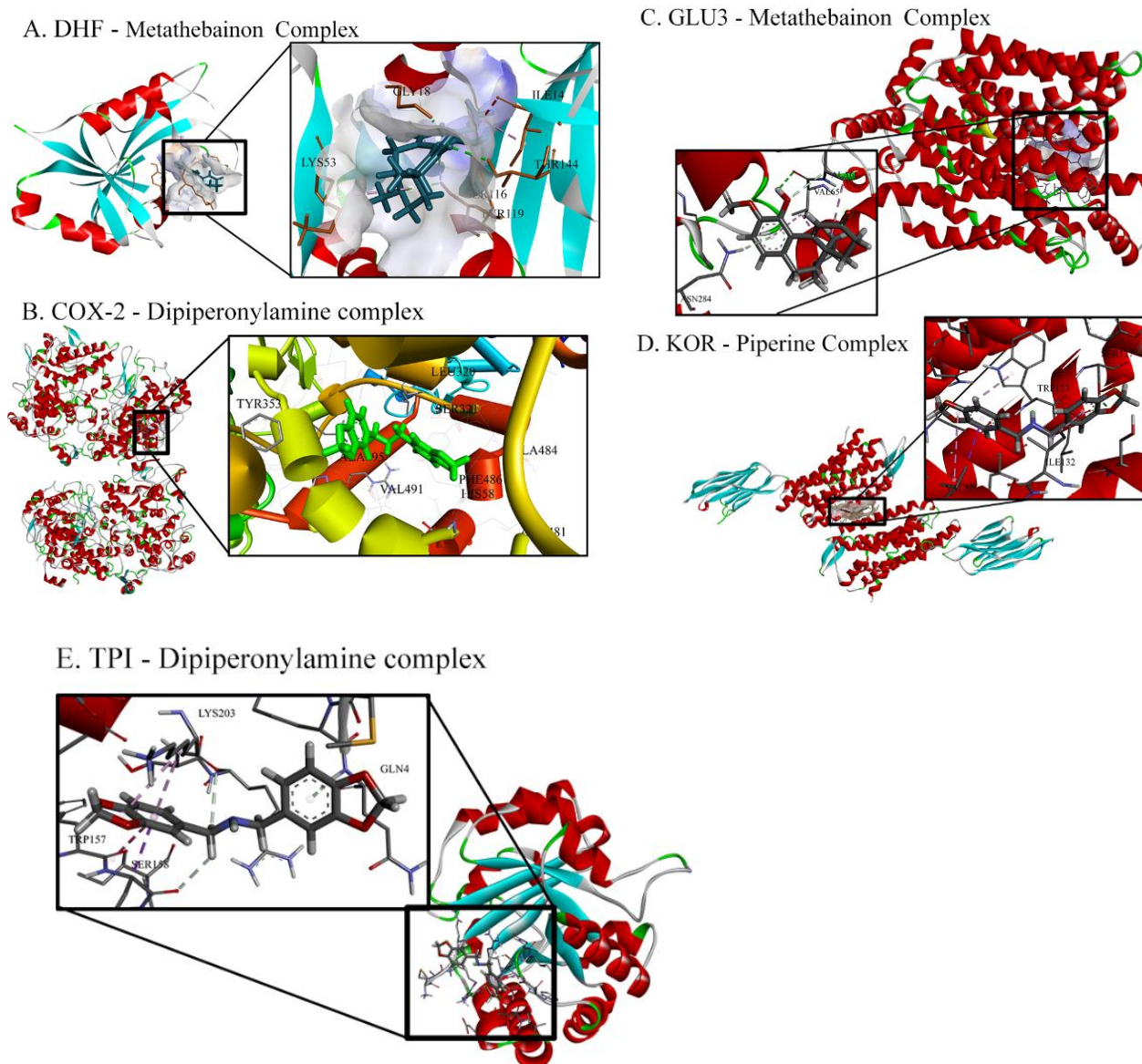
interactions with ALA A:66 and VAL A:285, along with multiple van der Waals contacts. In the case of the KOR–Piperine complex (Figs 3 D), the ligand exhibited strong interaction via a conventional hydrogen bond with SER B:127, supported by van der Waals bonds. Alkyl and π -alkyl interactions involving LEU A:125, TYR B:80, TRP B:123, ILE A:32, and VAL A:136 contributed to ligand stabilization within the receptor’s binding pocket. Lastly, the TPI–Dipiperonylamine complex (Figs 3 E) showed a diverse set of stabilizing interactions, including a π -sigma bond with SER A:158, a π -donor hydrogen bond with LYS A:203, and an amide– π stacked bond with TRP A:157. Carbon–hydrogen bonding with GLN A:4 and SER A:158, along with van der Waals interactions, supported the overall favorable binding conformation of the ligand.



Figs 2 – Validation of the molecular docking protocol by redocking native ligands (positive controls) into their respective macromolecular targets. (A) Cyclooxygenase-2 with its native ligand Protoporphyrin IX containing Fe; (B) DHFR with its cofactor NADPH (Dihydro-Nicotinamide-Adenine-Dinucleotide Phosphate); (C) Glucose Transporter 3 with Alpha-maltose; (D) Kappa-opioid receptor with Cholesterol. Superimposition of the redocked poses (grey) onto the co-crystallized native ligands (green) confirms the reliability of the docking parameters.

Table 4 The interactions between macromolecules and high-affinity ligands

Macromolecules/Ligands	Piperine	Dipiperonylamine	Metathebainon
DHFR	-8.552	-8.514	-8.658
COX-2	-8.368	-9.56	-7.985
GLUT3	-8.758	-8.755	-8.818
KOR	-9.549	-9.146	-9.048
TPI	-7.266	-7.773	-7.492



Figs 3 – 3D molecular interactions of high-affinity *E. ribes* compounds with therapeutic targets. (A) DHFR–Metathebainon complex; (B) COX-2–Dipiperonylamine complex; (C) GLUT3–Metathebainon complex; (D) KOR–Piperine complex; (E) TPI–Dipiperonylamine complex. Insets provide a magnified view of the ligand binding within the active site pocket (BIOVIA Discovery Studio Visualizer V24.1.0.23298).

Anticandidal Effect

The *in vitro* anticandidal activity of the *E. ribes* was qualitatively confirmed using the diameter of inhibition zones. The *E. ribes* exhibited varying degrees of antifungal activity as shown in Table 5 and Figs 4. A one-way ANOVA confirmed a statistically significant difference in antifungal potential among the treatment groups ($F(8, 18) = 39.17, p < 0.001$). Post-hoc analysis revealed that the FERM and FERC exhibited high inhibition zones (21.67 mm) that were statistically equivalent to the positive control (22.00 mm, $p = 1.000$), suggesting potent antifungal efficacy comparable to the standard drug. While the DERM also showed strong activity (20.33 mm), the DERE was significantly less effective ($p < 0.001$). Furthermore, no significant difference was observed between the crude and purified extracts ($p > 0.05$), indicating that purification did not enhance antimicrobial activity.

Table 5 Anticandidal activity of extracts of *E. ribes* against *C. albicans*.

Organism	DEREA	DEREA with purifier	DERM	DER _M with purifier	FERM	FERC	FEREA	FERCE	Control
<i>C. albicans</i> (mm)	14.3±0.5 ^f	14.6±1.1 ^f	20.3±0.5 ^{bc}	19.6±0.5 ^c	21.6±0.5 ^{ab}	21.6±1.1 ^{ab}	18±1.0 ^d	16.3±0.5 ^e	22±1.0 ^a

Values are expressed as mean ± SE (n = 3). Means followed by different superscript letters within the same row differ significantly (p < 0.05) according to Duncan's Multiple Range Test (DMRT). mm – millimeter.

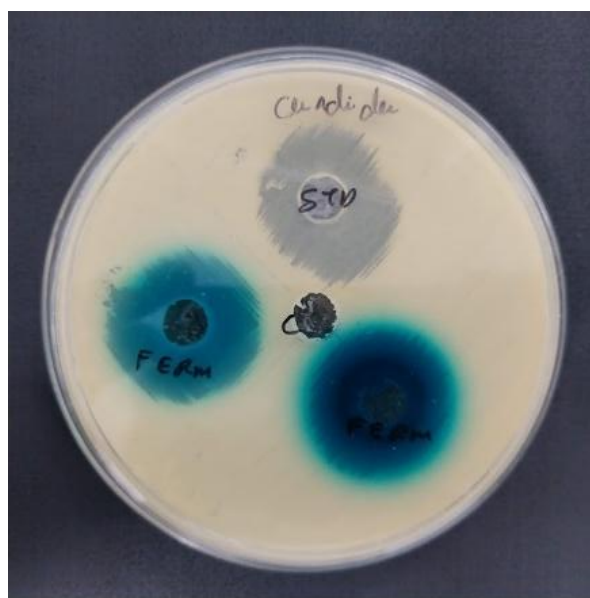


Fig. 4 – *In vitro* anticandidal activity of *Embelia ribes* extracts evaluated by agar well diffusion assay against *Candida albicans*. The image shows a representative agar plate from three independent experiments (n = 3) illustrating zones of inhibition produced by the fresh methanolic extract (FERM) in comparison with the positive control clotrimazole (STD).

Discussion

In this study, we integrated *in silico* analyses with *in vitro* assays to evaluate the antifungal potential of *Embelia ribes* extracts against *Candida albicans*. The PCA clustering (Figs 1-B) revealed a distinct separation between the fresh and dry *E. ribes* extracts. Biologically, this implies that the post-harvest drying process significantly alters the phytochemical profile of the seeds. The tight clustering of the fresh extracts (FERM and FEREA) distinctly different from the dry counterparts suggests that specific bioactive metabolites are either degraded or chemically transformed during drying. Furthermore, the divergent vectors for methanol and ethyl acetate in the PCA loading plot indicate that solvent polarity plays a critical role in retrieving these distinct metabolite profiles, highlighting the necessity of using fresh seeds for maximizing specific bioactive constituents. Among the extracts tested, the FERM produced the largest inhibition zone (21.6 ± 0.5 mm). These results are consistent with findings by Rani et al. (2011) and Thyloor (2018), underscoring the potent anticandidal activity of. GC-MS/MS profiling and subsequent molecular docking identified Piperine, Metathebainon, and Dipiperonylamine as the principal bioactive constituents, exhibiting high binding affinities toward COX-2, TPI, and KOR. Given the increasing prevalence of antifungal resistance, particularly among immunocompromised individuals, *E. ribes* extracts provide a viable alternative for therapeutic development. The demonstrated antifungal properties of Piperine suggest its potential inclusion in combination therapies to enhance efficacy and reduce resistance. Furthermore, the favorable safety profiles of

these compounds reinforce their suitability for clinical applications (Rani et al. 2011, Thyloor 2018, Bravo-Chaucanés et al. 2023).

Adherence to Lipinski's rule (Foudah et al. 2021) of five reinforced the drug-like profiles of Molecules 23 (Piperine), 114 (Dipiperonylamine), and 227 (Metathebainon), each showing favorable molecular weight, lipophilicity, and hydrogen-bonding parameters. ADMET predictions further indicated excellent intestinal absorption (human intestinal absorption > 90%, Caco-2 permeability > 1), minimal skin permeation ($\log K_p < -2.5$), and clean genotoxicity profiles (Ames-negative). Notably, Piperine and Dipiperonylamine had moderate blood-brain barrier penetration (BBB permeability ~ 0.27) but low CNS exposure ($\log PS < -1.6$). Clinically, this low CNS permeability presents a trade-off: while it advantageously minimizes the risk of central nervous system toxicity (Cornelissen et al. 2023), it also limits the utility of these compounds for treating invasive fungal infections that have disseminated to the central nervous system, such as *Candida* meningitis (Susan et al. 2025). Regarding metabolism, the inhibition of major cytochrome P450 enzymes (CYP2D6, CYP2C19, and CYP1A2) by these compounds suggests a potential for drug-drug interactions (Sarwar et al. 2024). In a clinical setting involving polypharmacy, the co-administration of *E. ribes* derived compounds could alter the pharmacokinetics of other drugs metabolized by these pathways, potentially leading to elevated plasma levels and toxicity. Consequently, future clinical applications would require careful dose optimization and therapeutic monitoring to mitigate these risks. None showed predicted Ames mutagenicity or skin sensitization, supporting favorable safety profiles. Piperine and Dipiperonylamine emerge as the most promising leads for further development as orally administered agents, whereas Metathebainon requires additional evaluation of its CNS effects and metabolic liabilities.

Our *in vitro* findings corroborate the docking predictions: FERM's high Piperine content (24.07% area) corresponds with the strongest activity. While a compelling correlation exists between the high Piperine content in FERM (24.07%) and its superior antifungal activity, the relationship is not strictly linear across all extracts. For instance, the DERM extract, despite containing a significant concentration of Piperine (15.17%), exhibited slightly lower efficacy. This discrepancy can be attributed to the physicochemical limitations of Piperine, specifically its extremely low water solubility (~ 0.055 mM) and susceptibility to degradation (Cho et al. 2025). In the fresh extract (FERM), Piperine likely exists in a naturally solubilized state, facilitated by the presence of other phytochemicals, which enhances its diffusion through the aqueous agar matrix. In contrast, the thermal processing involved in preparing the DERM may have induced thermal degradation or crystallization of Piperine, as free Piperine is known to be structurally unstable under heat and environmental stress (Chen et al. 2020). Consequently, this restricts its diffusion and subsequent antifungal impact in the dry extract despite its high initial abundance. The inhibition of TPI likely impairs fungal energy metabolism (Satala et al. 2021), whereas COX-2 inhibition may attenuate host inflammation during infection (Shrestha et al. 2020). Given rising azole resistance, such multifunctional agents could enhance therapeutic efficacy and curb resistance development.

Molecular docking validated the stability of the ligand-target complexes, with all RMSD values < 2 Å. The COX-2-Dipiperonylamine interaction was stabilized by hydrogen bonds to ARG 481 and HIS 58, and extensive hydrophobic contacts within the active site. Piperine likewise formed a key hydrogen bond with SER 127 of KOR, reinforced by π -alkyl interactions. Dipiperonylamine's π -sigma and amide- π stacking with TPI residues (TRP 157, SER 158) suggest effective disruption of fungal glycolysis. These dual antifungal-anti-inflammatory modes of action position Piperine and Dipiperonylamine as promising lead compounds. The findings of this study align with previous reports highlighting the antifungal and anti-inflammatory properties of Piperine and related bioactive compounds. Prior studies established Piperine's inhibitory effects on *C. albicans* and other fungal species, corroborating its potential as a therapeutic agent (Das et al. 2024). The observed COX-2 inhibition further supports its dual-action role, as demonstrated in other pharmacological investigations (Yu et al. 2024).

The utilization of *E. ribes* as a natural antifungal source presents significant environmental and economic advantages. Its sustainable cultivation and ease of extraction offer a cost-effective

alternative to synthetic antifungals. Furthermore, local production of *E. ribes* could stimulate regional economies while promoting traditional medicine practices (Patel et al. 2024).

While the study provides robust evidence of antifungal activity, certain limitations should be acknowledged. Molecular docking simulations are predictive in nature and require further validation through comprehensive *in vitro* and *in vivo* studies. Additionally, the bioavailability and pharmacological behavior of the identified compounds under physiological conditions remain to be established. Expanding the study to include other fungal pathogens will further elucidate the broad-spectrum potential of *E. ribes* extracts.

This study integrates chemical profiling, *in silico* modeling, and *in vitro* validation to highlight the antifungal potential of *E. ribes* extracts. Piperine, Metathebainon, and Dipiperonylamine emerged as key compounds with significant binding affinity and favorable pharmacokinetic attributes, supporting their advancement as oral antifungal agents. Further preclinical and mechanistic investigations are necessary to translate these findings into clinical applications.

Acknowledgements

We extend our sincere gratitude to the Shriram Research Institute, Bengaluru and the Indian Academy Degree College - Autonomous, Bengaluru, for providing the necessary support for this research.

Ethical Statement

This research involved *in silico* molecular docking and *in vitro* laboratory experiments using standardized microbial cultures obtained from the Microbial Type Culture Collection and Gene Bank (MTCC), India. As the study was limited to established laboratory strains and did not involve human participants, clinical samples, or animal subjects, formal ethical approval was not required.

References

- Arafat Md, Moon NJ, Mohammad M, Mamun MdJI et al. 2025 – Comprehensive Evaluation of Methanolic Fruits Extract of *Jatropha gossypifolia* L.: Neuropharmacological, Cytotoxic, Anthelmintic, GC–MS Profiling, and Molecular Docking Studies. *Pharmacology Research & Perspectives* 13, e70185. Doi 10.1002/prp2.70185.
- Bravo-Chaucanés CP, Chitiva LC, Vargas-Casanova Y, Diaz-Santoyo V et al. 2023 – Exploring the Potential Mechanism of Action of Piperine against *Candida albicans* and Targeting Its Virulence Factors. *Biomolecules* 13. Doi 10.3390/biom13121729.
- Chen S, Li Q, McClements DJ, Han Y et al. 2020 – Co-delivery of curcumin and piperine in zein-carrageenan core-shell nanoparticles: Formation, structure, stability and *in vitro* gastrointestinal digestion. *Food Hydrocolloids* 99, 105334. Doi 10.1016/j.foodhyd.2019.105334.
- Cho S, Jung Y, Rho S-J, Kim Y-R. 2025 – Stability, bioavailability, and cellular antioxidant activity of piperine complexed with cyclic glucans. *Food Science and Biotechnology* 34, 2475–2488. Doi 10.1007/s10068-025-01884-1.
- Cornelissen FMG, Markert G, Deutsch G, Antonara M et al. 2023 – Explaining Blood–Brain Barrier Permeability of Small Molecules by Integrated Analysis of Different Transport Mechanisms. *Journal of Medicinal Chemistry* 66, 7253–7267. Doi 10.1021/acs.jmedchem.2c01824.
- Das S, Malik M, Dastidar DG, Roy R et al. 2024 – Piperine, a phytochemical prevents the biofilm city of methicillin-resistant *Staphylococcus aureus*: A biochemical approach to understand the underlying mechanism. *Microbial Pathogenesis* 189, 106601. Doi 10.1016/j.micpath.2024.106601.

- Dela Peña RA, Sabeer Hussain MA, Danaphal A, Mohamed MD et al. 2025 – Phytochemical Screening, Radical Scavenging and Antimicrobial Activities of the Crude Ethanolic, Methanolic, Ethyl Acetate and Chloroform Leaf Extracts of Arayat Pitogo (*Cycas riuminiana* Porte ex Regel). Doi 10.1101/2025.06.21.656729.
- Foudah AI, Alqarni MH, Alam A, Salkini MA et al. 2021 – Determination of Chemical Composition, In Vitro and In Silico Evaluation of Essential Oil from Leaves of *Apium graveolens* Grown in Saudi Arabia. *Molecules* 26, 7372. Doi 10.3390/molecules26237372.
- Ghany LMAA, Ryad N, Abdel-Aziz MS, El-Lateef HMA et al. 2024 – Design, synthesis, antimicrobial evaluation, and molecular modeling of new sulfamethoxazole and trimethoprim analogs as potential DHPS/DHFR inhibitors. *Journal of Molecular Structure* 1309, 138170. Doi 10.1016/j.molstruc.2024.138170.
- Jeziorek M, Frej-Mądrzak M, Choroszy-Król I. 2019 – The influence of diet on gastrointestinal *Candida* spp. colonization and the susceptibility of *Candida* spp. to antifungal drugs. *Rocz Panstw Zakl Hig* 195–200. Doi 10.32394/rpzh.2019.0070.
- Khetagoudar MC, Chetti MB, Kumar AP, Bilehal DC. 2022 – Multiresidue Pesticide Analysis in Okra (Ladyfinger) Using Gas Chromatography Tandem Mass Spectrometry (GC-MS/MS). *Pesticide Toxicology* 53–64. Doi 10.1007/978-1-0716-1928-5_3.
- Leema Joseph, Nafeesth Beevi A, Jyothi.R. 2024 – An In Vitro Study on the Antimicrobial Effect of Fumigation with Jatu-Sarjarasadi Choorna. *International Journal of Research in Ayurveda and Pharmacy* 93–101. Doi 10.47070/ijapr.v12i1.3080.
- Mazri R, Ouassaf M, Kerassa A, Alhatlani BY. 2024 – Exploring potential therapeutics: Targeting dengue virus NS5 through molecular docking, ADMET profiling, and DFT analysis. *Chemical Physics Impact* 8, 100468. Doi 10.1016/j.chphi.2024.100468.
- mcs07 2016 – PubChemPy documentation.
- Patel M, Alnajjar LI, Alomrani SO, Alshammari N et al. 2024 – *Embelia ribes* Burm.f. fruit extract inhibit quorum sensing-dependent production of virulence factors and biofilm formation: An integrated in vitro and in silico approach. *South African Journal of Botany* 165, 307–323. Doi 10.1016/j.sajb.2024.01.002.
- Prakash V, Giri KR, Palandurkar KM, Banerjee T et al. 2024 – Preliminary evaluation of in-Vivo and in-Vitro antifungal activity of *Piper longum*, *Origanum majorana*, *Embelia ribes* and *Butea monosperma* with Gas chromatography-mass spectrometry analysis of phytochemical property of plant extracts against *Candida* species causing dermatological. *IP Indian Journal of Clinical and Experimental Dermatology* 10, 11–18. Doi 10.18231/j.ijced.2024.002.
- Rani AS, Saritha K, Nagamani V, Sulakshana G. 2011 – In vitro Evaluation of Antifungal Activity of the Seed Extract of *Embelia Ribes*. *Indian Journal of Pharmaceutical Sciences* 73, 247–249.
- Sarwar MF, Zahra A, Awan MF, Ali S et al. 2024 – Assessing the efficacy of cinnamon compounds against *H. pylori* through molecular docking, MD Simulations and ADMET analyses. *PLoS ONE* 19, e0299378. Doi 10.1371/journal.pone.0299378.
- Satala D, Satala G, Zawrotniak M, Kozik A. 2021 – *Candida albicans* and *Candida glabrata* triosephosphate isomerase – a moonlighting protein that can be exposed on the candidal cell surface and bind to human extracellular matrix proteins. *BMC Microbiology* 21, 199. Doi 10.1186/s12866-021-02235-w.
- Sehrawat R, Rathee P, Khatkar S, Akkol E et al. 2024 – Dihydrofolate Reductase (DHFR) Inhibitors: A Comprehensive Review. *Current Medicinal Chemistry* 31, 799–824. Doi 10.2174/0929867330666230310091510.
- Shrestha S, Kim M-J, Eldridge M, Lehmann ML et al. 2020 – PET measurement of cyclooxygenase-2 using a novel radioligand: upregulation in primate neuroinflammation and first-in-human study. *Journal of Neuroinflammation* 17, 140. Doi 10.1186/s12974-020-01804-6.

- Susan V, Lang M, Sabou M, Bourel-Bonnet L. 2025 – Antifungal Drugs for the Treatment of Invasive Fungal Infections—A Limited Therapeutic Toolbox Facing Growing Resistances. *Pharmaceuticals* 18, 1220. Doi 10.3390/ph18081220.
- Taher MA, Laboni AA, Islam MA, Hasnat H et al. 2024 – Isolation, characterization and pharmacological potentials of methanol extract of *Cassia fistula* leaves: Evidenced from mice model along with molecular docking analysis. *Heliyon* 10, e28460. Doi 10.1016/j.heliyon.2024.e28460.
- Tahil G, Delorme F, Le Berre D, Monflier É et al. 2023 – Curated dataset of association constants between a cyclodextrin and a guest for machine learning. *Chemical Data Collections* 45, 101022. Doi 10.1016/j.cdc.2023.101022.
- Thyloor R. 2018 – Phytochemical analysis of *Embelia ribes* seeds for antimicrobial activities. *Journal of Medicinal Plants* 6, 41–43.
- Wang X, Li M, Yang Y, Shang X et al. 2024 – Clinical significance of inflammatory markers for evaluating disease severity of mixed-pathogen bloodstream infections of both *Enterococcus* spp. and *Candida* spp. *Heliyon* 10, e26873. Doi 10.1016/j.heliyon.2024.e26873.
- Yu L, Hu X, Xu R, Zhao Y et al. 2024 – Piperine promotes PI3K/AKT/mTOR-mediated gut-brain autophagy to degrade α -Synuclein in Parkinson's disease rats. *Journal of Ethnopharmacology* 322, 117628. Doi 10.1016/j.jep.2023.117628.